

IN SEARCH FOR A SAT-FRIENDLY BINARIZED NEURAL NETWORK ARCHITECTURE.

Anonymous authors

Paper under double-blind review

ABSTRACT

Analyzing the behavior of neural networks is one of the most pressing challenges in deep learning. Binarized Neural Networks are an important class of networks that allow equivalent representation in Boolean logic and can be analyzed formally with logic-based reasoning tools like SAT solvers. Such tools can be used to answer existential and probabilistic queries about the network, perform explanation generation, etc. However, the main bottleneck for all methods is their ability to reason about large BNNs efficiently. In this work, we analyze architectural design choices of BNNs and discuss how they affect the performance of logic-based reasoners. We propose changes to the BNN architecture and the training procedure to get a simpler network for SAT solvers without sacrificing accuracy on the primary task. Our experimental results demonstrate that our approach scales to larger deep neural networks compared to existing work for existential and probabilistic queries, leading to significant speed ups on all tested datasets.

1 INTRODUCTION

Deep neural networks are among the most successful AI technologies making impact in a variety of practical applications ranging from vision to speech recognition and natural language (Goodfellow et al., 2016). However, many concerns have been raised about the decision making process behind machine learning technology. For instance, can we trust decisions that neural networks make (EU Data Protection Regulation, 2016; Goodman & Flaxman, 2017; NIPS IML Symposium, 2017)? One way to address this problem is to define properties that we expect the network to satisfy. Verifying whether the network satisfies these properties sheds light on the properties of the function that it represents. Verification guarantees can reassure the user that the network behaves as expected.

There are two main approaches to neural network analysis. The first approach, the *certification* of neural networks, trains a verified network that satisfies given properties, e.g. a network that is guaranteed to be robust to adversarial perturbations (Wong & Kolter, 2018; Dvijotham et al., 2018; Raghunathan et al., 2018; Mirman et al., 2018). However, a set of properties must be known in advance, which might not always be possible. Moreover, enforcing a set of properties during the training procedure can significantly affect the accuracy of the network on the primary task. Finally, certification techniques work with relaxation of the original problem and might not be able to certify robust inputs. The second approach, the *verification* of neural networks, takes a trained network as input and focuses only on the verification task (Katz et al., 2017; Weng et al., 2018; Singh et al., 2019; Xiao et al., 2019). A number of verification frameworks were proposed over the last few years that can be roughly divided into complete (Katz et al., 2017; 2019; Tjeng et al., 2019) and incomplete methods (Weng et al., 2018; Zhang et al., 2018; Singh et al., 2018). As the training and verification tasks are separated, a wide set of properties can be checked. However, the scalability of this approach remains an issue, especially for complete methods.

In this work we tackle the scalability problem of the complete verification approach, in the context of an important class of networks, Binarized Neural Networks (BNNs) (Hubara et al., 2016). A BNN is an extreme case of quantized neural networks where parameters are primarily binary. These networks have a number of important features that are useful in resource constrained environments, like embedded devices or mobile phones (McDanel et al., 2017; Kung et al., 2017). They are memory efficient as only one bit per weight must be stored and are computationally efficient as all activations are binary, which enables the use of specialized algorithms for fast binary matrix multiplication.

Structure of i th internal block, $\text{BLOCK}_i : \{-1, 1\}^{n_i} \rightarrow \{-1, 1\}^{n_{i+1}}$ on input $x^i \in \{-1, 1\}^{n_i}$	
LIN	$y = A^i x^i + b^i$, where $A^i \in \{-1, 1\}^{n_{i+1} \times n_i}$ and $b^i \in \mathbb{R}^{n_{i+1}}$
BN	$z_t = \alpha_t^i \left(\frac{y_t - \mu_t^i}{\sigma_t^i} \right) + \gamma_t^i$, where $y = (y_1, \dots, y_{n_{i+1}})$, and $\alpha_t^i, \gamma_t^i, \mu_t^i, \sigma_t^i \in \mathbb{R}$
BIN	$x^{i+1} = \text{sign}(z)$, where $z = (z_1, \dots, z_{n_{i+1}}) \in \mathbb{R}^{n_{i+1}}$, and $x^{i+1} \in \{-1, 1\}^{n_{i+1}}$
Structure of the output block, $\text{OUTPUT} : \{-1, 1\}^{n_d} \rightarrow \mathbb{R}^p$ on input $x^d \in \{-1, 1\}^{n_d}$	
LIN	$o = Cx^d + q$, where $C \in \{-1, 1\}^{p \times n_d}$ and $q \in \mathbb{R}^p$

Table 1: Structure of internal and output blocks, which, stacked together, form a BNN.

More importantly, these networks admit exact representation in Boolean logic (Narodytska et al., 2018; Cheng et al., 2018). Such a representation enables us to apply powerful Boolean reasoning tools to the analysis of BNNs. For example, we can perform a rich set of queries, ranging from existential queries (e.g., is there a faulty input to the network?), to counting queries (e.g., how many faulty inputs exist?), using logic-based reasoners (Baluta et al., 2019; Shih et al., 2019).

This paper makes two main contributions. First, we analyze how different architectural design choices for BNNs affect the performance of SAT solvers. To identify influential parts of the design, we scrutinize BNNs at three levels of granularity: individual neurons, blocks of layers, and network as a whole. Our work continues work of Narodytska et al. (2018) and Cheng et al. (2018) where BNNs were analyzed on the network level. Here we put our focus on individual neurons and blocks. Second, we exploit our findings to train SAT-friendly BNNs. We propose a modified training procedure that makes the resulting network easier for logic-based verification tools, like SAT solvers, to reason about. Modifications to training are crucially performed so that the accuracy of the network is unaffected. Overall, our approach (a) preserves the separation between training and verification, by not committing to a certain property during training and (b) boosts the performance of logic-based verification. We implemented the proposed methods and demonstrated significant performance gains over previous work (Narodytska et al., 2018; Khalil et al., 2019; Baluta et al., 2019). We get more than 10x-20x improvements on tested benchmarks for both verification and quantitative queries, e.g., finding the probability that a perturbation yields an adversarial example.

2 BACKGROUND

Boolean satisfiability (SAT). We assume notation and definitions standard in Boolean Satisfiability (SAT), i.e. the decision problem for propositional logic (Biere et al., 2009). SAT formulas are defined over a set of Boolean variables $\{\mathbf{x}_1, \dots, \mathbf{x}_n\}$. A literal l_i is a variable \mathbf{x}_i (‘positive’ polarity) or its complement $\bar{\mathbf{x}}_i$ (‘negative’ polarity). *Cardinality constraints* over Boolean variable are constraints of the form $\sum_{i=0}^n l_i \geq k$, where $l_i \in \{\mathbf{x}_i, \bar{\mathbf{x}}_i\}$. In this work we employ *reified cardinality constraints*: $\mathbf{x}' \Leftrightarrow \sum_{i=0}^n l_i \geq k$. We use the full sequential counters encoding (Sinz, 2005b) to model this constraint in SAT. We also work with (approximate) solutions counting solvers, e.g. ApproxMC3. See details on such methods in Appendix A.

Binarized neural networks We summarise standard BNN structure (Hubara et al., 2016). A BNN consists of blocks of layers, each mapping binary vectors to binary vectors. We define a *block* (referred to as BLOCK) as a function mapping an input to an output, i.e., $\text{BLOCK}^i : \{-1, 1\}^{n_i} \rightarrow \{-1, 1\}^{n_{i+1}}$, $i = 1, \dots, d-1$, where $d-1$ is the number of hidden layers. The last block, denoted OUTPUT , has a slightly different structure: $\text{OUTPUT} : \{-1, 1\}^{n_d} \rightarrow \mathbb{R}^p$, where p is the number of outputs of the network. Each BLOCK takes an input vector x and applies three transformations: a linear transformation (LIN), batch normalization (BN) and binarization (BIN)¹. Table 1 shows transformations of internal and output blocks in detail.

3 LOGIC-BASED ANALYSIS OF BNNs

An important property of BNNs is that they allow exact encoding into SAT: for each BNN there exists a SAT formula such that solutions of the formula are exactly the set of all valid input/output pairs of the BNN (Narodytska et al., 2018; Cheng et al., 2018). Such translation opens many possibilities for logic-based analysis of BNNs. In this section, we describe several such methods. We highlight

¹In the training phase, there is an additional *hard* tanh layer after batch normalization, but it is redundant in the inference phase.

that reasoning tools available for BNNs are more diverse and powerful compared to frameworks available for the analysis of conventional networks, which focus mostly on verification and certification of NNs. Since logic-based analysis of BNNs exploits their logical representation, we start by revisiting how to obtain such a representation before discussing logic-based BNN analysis tools.

3.1 SAT ENCODING OF BNNs

We consider how to generate a logical encoding of a BNN (Narodytska et al., 2018). Consider a single block BLOCK^i , which applies three transformations: LIN, BN and BIN to the input vector. We will use the following running example to demonstrate the encoding.

Example 3.1. Consider a block with three inputs and two outputs. We define transformation parameters as follows: LIN : $A = [1, -1, 1; -1, -1, 1]$, $b = [0, 0]$ and BN : $\alpha = [0.1, 0.1]$, $\mu = [1, -1]$, $\sigma = [1, 1]$, $\gamma = [0.1, 0.2]$. \square

We encode these transformations as a system of logic constraints. We introduce a vector of binary variables $x^i \in \{-1, 1\}^{n_i}$ to encode inputs and $x^{i+1} \in \{-1, 1\}^{n_{i+1}}$ to encode outputs of BLOCK^i . Since transformations are applied sequentially, we can encode the block as their composition:

$$x_j^{i+1} = \text{sign} \left(\frac{\alpha_j^i}{\sigma_j^i} \left(\sum_{t=1}^{n_i} a_{j,t}^i x_t^i + b_j^i - \mu_j^i \right) + \gamma_j^i \right), j = 1 \dots n_{i+1}, \quad (1)$$

where $a_{j,t}^i$ and b_j^i are parameters of LIN, $\alpha_j^i, \sigma_j^i, \mu_j^i$ and γ_j^i are parameters of BN. To obtain a SAT encoding, we need to eliminate binary variables as a SAT formula is defined over Boolean variables. We introduce Boolean variables $\mathbf{x}_t \in \{0, 1\}$, $t = 1, \dots, n_i$ and relate them to the corresponding binary variables x_t : $x_t = 2\mathbf{x}_t - 1$, $t = 1, \dots, n_i$. We get that if $\mathbf{x}_t = 0$ then $x_t = -1$, otherwise $x_t = 1$. We can now rewrite the last expression as $\mathbf{x}_j^{i+1} = \text{sign} \left(\frac{\alpha_j^i}{\sigma_j^i} \left(\sum_{t=1}^{n_i} a_{j,t}^i 2\mathbf{x}_t^i - \sum_{t=1}^{n_i} a_{j,t}^i + b_j^i - \mu_j^i \right) + \gamma_j^i \right)$, $j = 1 \dots n_{i+1}$. We denote $C_j = \left(-\sum_{t=1}^{n_i} a_{j,t}^i + b_j^i - \mu_j^i \right)$, as these are just constants. We get

$$\mathbf{x}_j^{i+1} \Leftrightarrow \begin{cases} \sum_{t=1}^{n_i} a_{j,t}^i \mathbf{x}_t^i \geq \frac{-\gamma_j^i \sigma_j^i}{2\alpha_j^i} - \frac{C_j}{2}, & \text{if } \alpha_j^i > 0 \\ \sum_{t=1}^{n_i} a_{j,t}^i \mathbf{x}_t^i \leq \frac{-\gamma_j^i \sigma_j^i}{2\alpha_j^i} - \frac{C_j}{2}, & \text{if } \alpha_j^i < 0 \\ \gamma_j^i \geq 0, & \text{if } \alpha_j^i = 0. \end{cases}, j = 1 \dots n_{i+1}, \quad (2)$$

Example 3.2. Consider how the encoding works on Example 3.1. We introduce three binary variables to encode inputs x_i^0 , $i = 0, 1, 2$, and two binary variables to encode outputs x_0^1 and x_1^1 . Inputs and outputs are connected as follows:

$$x_0^1 = \text{sign}(0.1(x_0^0 - x_1^0 + x_2^0 - 1) + 0.1 \geq 0); x_1^1 = \text{sign}(0.1(-x_0^0 - x_1^0 + x_2^0 + 1) + 0.2 \geq 0).$$

Next we perform variable replacement as explained above using the relation $x_t = 2\mathbf{x}_t - 1$. Note that α_1^0 and α_2^0 are both positive so we get:

$$\mathbf{x}_0^1 \Leftrightarrow (0.1(2\mathbf{x}_0^0 - 1 - (2\mathbf{x}_1^0 - 1) + 2\mathbf{x}_2^0 - 1 - 1) + 0.1 \geq 0) \Leftrightarrow (\mathbf{x}_0^0 - \mathbf{x}_1^0 + \mathbf{x}_2^0 \geq 1/2),$$

$$\mathbf{x}_1^1 \Leftrightarrow (0.1(-(2\mathbf{x}_0^0 - 1) - (2\mathbf{x}_1^0 - 1) + 2\mathbf{x}_2^0 - 1 + 1) + 0.2 \geq 0) \Leftrightarrow (-\mathbf{x}_0^0 - \mathbf{x}_1^0 + \mathbf{x}_2^0 \geq -4/2). \quad \square$$

The final step is to encode reified cardinalities using Boolean variables instead of binary (integer) variables in Equation 2. We recall the following tautology for a Boolean variable $\mathbf{x}_t + \bar{\mathbf{x}}_t = 1$, where $\bar{\mathbf{x}}_t$ is a negation of \mathbf{x}_t . As all coefficients $a_{j,t}^i \in \{-1, 1\}$, Equation 2 contains linear constraints with unary coefficients (see the last transformation in Example 3.2). We denote $N_j = |\{a_{j,t}^i < 0, t = 1, \dots, n_{i+1}\}|$ the number of negative coefficients in the j th row and assume $\alpha_j^i \neq 0$.

$$\mathbf{x}_j^{i+1} \Leftrightarrow (l_1^i + \dots + l_{n_i}^i \geq h_j), \quad (3)$$

$$\text{where } l_t^i = \begin{cases} \mathbf{x}_t^i & \text{if } a_{j,t}^i \geq 0 \\ \bar{\mathbf{x}}_t^i & \text{if } a_{j,t}^i < 0 \end{cases} \text{ and } h_j = \begin{cases} \lceil -\gamma_j^i \sigma_j^i / (2\alpha_j^i) - C_j / 2 - N_j \rceil & \text{if } \alpha_j^i > 0 \\ \lfloor -\gamma_j^i \sigma_j^i / (2\alpha_j^i) - C_j / 2 - N_j \rfloor & \text{if } \alpha_j^i < 0. \end{cases}$$

We recall that a constraint of type Equation 3 is a *reified cardinality constraint* that can be translated into Boolean formulae (Sinz, 2005b). We refer to a SAT encoding of BLOCK as $\text{BINBLOCK}^i(\mathbf{x}^i, \mathbf{x}^{i+1})$. Similarly, we can encode the OUTPUT block (Appendix B). We can now represent the entire network as a Boolean formula: $\text{BINBNN}(\mathbf{x}, o) \equiv \bigwedge_{i=1}^{d-1} \text{BINBLOCK}^i(\mathbf{x}^i, \mathbf{x}^{i+1}) \wedge \text{BINOUTPUT}(\mathbf{x}^d, o)$, where $\text{BINBLOCK}^i(\mathbf{x}^i, \mathbf{x}^{i+1})$ encodes the i th block BLOCK^i with input \mathbf{x}^i and output \mathbf{x}^{i+1} , $i \in [0, d-1]$, $\text{BINOUTPUT}(\mathbf{x}^d, o)$ is a Boolean encoding of the last layer.

3.2 BNN’S REASONERS

We consider three types of reasoners designed for BNNs. The first type includes property checkers that can handle existential queries, e.g. ‘is there an input of the network that violates a given property?’. The second type deals with probabilistic queries, e.g. ‘what is an approximate probability that a valid input will violate a given property?’. Finally, the most powerful reasoner answers a large set of queries, like generating explanations, finding exact probabilities of property violations, etc.

Property checkers. Property checking of BNNs using a SAT-based approach was proposed in (Narodytska et al., 2018; Cheng et al., 2018). Given a precondition $prec$ on the inputs \mathbf{x} and a property $prop$ on the outputs o , we check if the following statement is valid: $prec(\mathbf{x}) \wedge \text{BINBNN}(\mathbf{x}, o) \Rightarrow prop(o)$. To decide if there exists a counterexample to this property, we look for a model of: $prec(\mathbf{x}) \wedge \text{BINBNN}(\mathbf{x}, o) \wedge \neg prop(o)$. An example of property checking is to check for the existence of adversarial perturbations. In this case, $prec$ defines an ϵ -ball of valid perturbations and $prop$ states that the classification should not change under small perturbations. An optimization version of this problem was considered in (Khalil et al., 2019) using ILP rather than SAT solvers.

Quantitative reasoners. In many practical applications, it is not sufficient to check for the existence of a counterexample to a given property. We would like to know precise or approximate probability of the undesired behavior. (Baluta et al., 2019), proposes a framework to answer such probabilistic queries using approximate model counting tools. The main technical challenge is to perform efficient approximate solution counting of a SAT formula that contains a BINBNN as a sub-formula. Consider the property verification formula above. By approximately counting solutions, we obtain an estimate of the probability of a valid input leading to a property violation with a controllable and bounded error². Baluta et al. (2019) identified three applications of this framework in the security domain: robustness, trojan attacks, and fairness. Narodytska et al. (2019) investigated how a similar type of quantitative reasoning can be used to assess the quality of ML explanations.

Knowledge compilation engines. The compilation of BNNs is an interesting research direction that aims to compile a BINBNN into a tractable structure, a logic graph-based representation of the formula (Shih et al., 2019; Choi et al., 2019) that supports a wide range of queries about the original BNN, including exact solution counting for probabilistic queries or generating logical explanations for network decisions. Interestingly, BNNs often admit succinct representations as the networks contain redundancies that can be eliminated by compilation. For example, (Choi et al., 2019) reports large reduction in the representation size on some benchmarks.

As can be seen from this overview, the success of these applications depends on the ability to reason efficiently about the underlying formula in the corresponding logical reasoner, e.g., a SAT solver, an approximate model counting method, or a knowledge compilation engine. On the one hand, BNNs are potentially easier to reason about compared to full-precision networks³. On the other hand, SAT is a hard combinatorial problem. Hence, developing efficient decision procedures require exploiting the special structure of BNNs.

4 ANALYSIS OF BNN’S FROM THE SAT STANDPOINT

In this section we analyze the properties of the formula BINBNN from the perspective of a solver developer. We discuss how these properties affect solver performance both positively and negatively. We highlight parts of the BNN architecture that can be exploited to speed up logical reasoners. To structure our analysis, we consider BNN’s at three levels of granularity that naturally correspond to sub-formulas of BINBNN. (Narodytska et al., 2018; Cheng et al., 2018; Khalil et al., 2019) discussed and exploited properties of BNNs on the highest level of granularity, but we believe that there are more opportunities to take advantage of the structure if we look at all levels systematically.

Neuron level We start with the level of an individual neuron. Recall that the value of a neuron is determined by Equation 3. Let us examine it in more detail. We note that A is a *dense matrix* by design as all entries must be 1 or -1 . At the same time, the number of literals in Equation 3 is equal to the width of A for fully-connected layers or the filter size for convolutional layers. Therefore, the high density of A leads to a large number of variables in the cardinality constraint of Equation 3. To

²The error bounds depend on the parameters of the model counting algorithm.

³For example, dealing with high-precision floating-point arithmetic requires specialized tools.

make things worse, depending on the encoding, the number of auxiliary variables to encode Equation 3 depends on n_i and h_j , e.g., the number of auxiliary variables introduced is $O(n_i h_j)$ for the sequential counters encoding, leading to large SAT representations. Hence, dense matrices lead to large encodings. Next, consider the logical structure of Equation 3. Note that we have an *equivalence relation* between the value of the neuron and the cardinality constraint. A key component of a SAT solver is the inference procedure, that at each point of the search infers values of unassigned variables. Suppose that we have a constraint $\mathbf{x}_1^1 \Leftrightarrow (\bar{\mathbf{x}}_0^0 + \bar{\mathbf{x}}_1^0 + \mathbf{x}_2^0 \geq 2)$. Moreover, suppose \mathbf{x}_0^1 has not been fixed yet and $\mathbf{x}_0^0 = 1$. Note that any setting of variables $\mathbf{x}_1^0, \mathbf{x}_2^0$ can be extended to a valid assignment in this constraint. Hence, no inference is possible. In contrast, assume we only had cardinality constraints, i.e. $\bar{\mathbf{x}}_0^0 + \bar{\mathbf{x}}_1^0 + \mathbf{x}_2^0 \geq 2$, then we can infer that $\mathbf{x}_1^0 = 0$ and $\mathbf{x}_2^0 = 1$ at this point. As the vast majority of constraints in the encoding contain the equivalence relation, this hinders the inference algorithm’s ability to find implied variables, making the solver dive deep before a conflict occurs.

Block level Next we go up one level of granularity and focus on the encoding of BLOCK. Consider our running Example 3.2. A block is encoded by a set of constraints over the same variables: $\mathbf{x}_0^0, \mathbf{x}_1^0$ and \mathbf{x}_2^0 in our example. We count over these variables therefore multiple times. This observation hints at an opportunity to identify shared computations and exploit them to get more succinct encodings. Note that in our running example, we encode the partial sum $-\mathbf{x}_1^0 + \mathbf{x}_2^0$ for both constraints and this can be shared. Our ability to share computations depends on the patterns in which 1 and -1 appear in the matrix A as these coefficients control whether variables appear positively or negatively in each constraint. As A is a full matrix and *no patterns are enforced* on occurrences of 1 and -1 between rows the amount of sharing is rather small for the standard BNN architecture.

Network level Finally, we consider the entire BNN as a chain of blocks. As each block is encoded individually, BINBNN is a conjunction of BINBLOCK formulas that are loosely connected via variables $\mathbf{x}^i, i = 1, \dots, d - 1$. As discussed above, \mathbf{x}^i variables are a small fraction of the total number of variables. Two factors affect solver performance. First, the block-wise structure of the BINBNN formula suggests that *formula decomposition* can be exploited by the solver. Second, the BINBNN formula effectively simulates the network function for all possible inputs. Additional constraints on inputs/outputs of the network, e.g., in the verification problem in Section 3.2, are the main source of inconsistencies. Therefore, conflict-driven learning, which is the core of all SAT solvers, should perform *directed search*, starting from either the last or the first blocks of the formula moving toward the first (last) blocks as search progresses rather than jumping unguided between layers. Such guidance might help to discover conflicts faster.

5 TOWARD SAT-FRIENDLY BNNs

We discuss how alternative architectural design choices for BNNs can be used to take advantage of the identified properties to reason faster. We observe that, assuming a fixed network architecture, our design options are limited. We therefore make an important assumption that we can change the architecture of the BNN and have access to the training procedure. While this is a strong assumption, we believe that BNN designers will be willing to incorporate changes into the training procedure as long as they do not cause accuracy loss. As before, we structure our solutions and observations using different levels of granularity.

Neuron level As discussed above, there are two properties of Equation 3 that need to be addressed. First issue is that A is a dense matrix by design of BNNs. To deal with this issue, we propose using a ternary quantization procedure instead of a binary quantization to learn sparse matrices for linear transformations. We recall that BNN is trained using two matrices: a full-precision matrix W^i that is updated during the gradient descent and a binarized matrix A^i , connected as follows $A^i = \text{sign}(W^i)$. A^i is used on the forward path and during inference. The modification we make is a simple two-sided ternary quantization of A^i during training:

$$a_{jt}^i = \begin{cases} \text{sign}(w_{jt}^i) & \text{if } |w_{jt}^i| \geq T, \\ 0 & \text{otherwise,} \end{cases} \quad (4)$$

where T is a parameter. In principle, T can be a learnable parameter (Zhu et al., 2017). However, in (Darabi et al., 2018), it was observed that weights of W are naturally grouped around points $-1, 1$ and 0 during training. Therefore, we use a fixed threshold T , obtained from the distribution of weights of a trained vanilla BNN. Allowing zero weights in A requires some modifications in the

original encoding of the last layer that we discuss in Appendix B. Consider how ternary quantization helps to reduce the encoding in our example.

Example 5.1. Consider Example 3.1. Suppose that after using ternary quantization the first row of A is $[1, 0, 0]$. Then we can make the following simplification: $x_0^1 = \text{sign}(0.1(x_0^0 - 1) + 0.1 \geq 0)$. By replacing with Booleans, we get $x_0^1 \Leftrightarrow (0.1(2x_0^0 - 1 - 1) + 0.1 \geq 0) \Leftrightarrow (x_0^0 \geq 1)$. The obtained reified cardinality constraint is much smaller in terms of the number of variables involved. In our experiments, a large fraction of coefficients can be reduced to 0 without hurting the accuracy. \square

The second issue at this level is that SAT solver inference is weak due to equivalence relations. Here we take the stabilization approach proposed in (Xiao et al., 2019) and adjust it to work for BNNs. The idea is to perform bounds propagation of the input bounds through the network to estimate lower and upper bounds of each linear constraint from Equation 1. We denote z_j^i the input of sign in Equation 1, so $z_j^i = (\alpha_j^i (\sum_{t=1}^{n_i} a_{j,t}^i x_t^i + b_j^i - \mu_j^i)) / (\sigma_j^i + \gamma_j^i)$ (See Appendix C for more details and an example). If $\text{sign}(ub(z_j^i)) = \text{sign}(lb(z_j^i))$ then the sign operator is stable in the sense that we know the value of x_j^{i+1} , e.g. if both bounds are positive then $x_j^{i+1} = 1$, otherwise -1 . For stable neurons, we can remove the equivalence relation and fix x_j^{i+1} simplifying the encoding.

Estimates of lower and upper bounds must be binarized as the bounds computation goes across BLOCKS. To mimic the computation flow on the bounds computation path, we apply *hard* tanh before the sign operator: $lb(x_i^{i+1}) = \text{sign}(\text{HARDTANH}(lb(z_j^i)))$ and $ub(x_i^{i+1}) = \text{sign}(\text{HARDTANH}(ub(z_j^i)))$. We must also take into account that parameters of the BN layer are learned in a different way. Namely, μ_j^i and σ_j^i are computed from the batch of samples, while other parameters are learned via gradient descent (Ioffe & Szegedy, 2015). When we compute bounds, we pass them through the BN layer, but we should exclude these fake inputs from the computation of μ_j^i and σ_j^i . Finally, to achieve the effect of stabilization during training, for each neuron, we encourage $ub(z_j^i)$ and $lb(z_j^i)$ to take the same sign by adding an extra term to the loss function that approximates $\text{sign}(ub(z_j^i)) \text{sign}(lb(z_j^i))$ as $-\tanh(1 + ub(z_j^i)lb(z_j^i))$ (Xiao et al., 2019).

Block level We recall that the main issue we identified is that it is not obvious how to take advantage of shared partial computations in constraints of a block. One solution could be to enforce a pattern of zero and non-zero coefficients for each matrix A . A recent and successful example of this is a butterfly matrix (Dao et al., 2019b;a). This is a structured matrix with a predefined sparsity pattern. The original matrix is replaced with a composition of highly sparse matrices of a rigid structure that provides a very good approximation of the original matrix (Dao et al., 2019a). This new matrix can potentially be used to create a natural decomposition of our block constraints. However, it is a matter of future research if butterfly matrices can be used alongside quantization. Another solution that we can use is a different binary quantization, e.g. $-1/0$ or $0/1$, for each row of the matrix instead of ternary quantization. This will ensure that variables either occur in the negative/positive polarity or are absent in each constraint. Keeping the same polarity per constraint may foster shared computations. However, the distribution of zeroes is also important here to get a good level of sharing. Hence, we believe that using predefined patterns might be more promising.

Network level Recall that we found two avenues for optimizing encoding at the network level: *formula decomposition* and *directed search*. In (Narodytska et al., 2018; Cheng et al., 2018), decomposability of BINBNN was exploited in limited forms there the authors independently proposed using CEGAR-like search to reason about property verification. (Khalil et al., 2019) took advantage of both decomposition and directed search by proceeding from the last to the first layer for a similar problem. However, while all these ideas appear to be helpful, there is no solver designed to incorporate such techniques. On the other hand, a number of verification frameworks exploit similar domain properties for bounded model checking (Bradley, 2011; Gurfinkel et al., 2015). So, it would be interesting to see if these solvers can be adapted for property verification of ML models.

6 EXPERIMENTS

We focus on the improvements we proposed for the neuron level of granularity. We use three datasets from (Narodytska et al., 2018; Baluta et al., 2019; Khalil et al., 2019). For each, we experiment with two tasks. First, we check if there is an untargeted adversarial attack (Goodfellow et al., 2015).

BNNs	MNIST		FASHION		MNISTBG	
	%	#prms	%	#prms	%	#prms
Vanilla	96.5	623K	82.1	623K	74.3	623K
Sparse	96.4	32K	84.1	37K	78.2	41K
Sparse+Stable	95.9	32K	83.2	37K	78.3	38K
Sparse+L1	96.0	20K	83.7	35K	78.4	36K
Sparse+L1+Stable	95.2	20K	82.9	37K	80.0	34K

Table 2: The test accuracy (%) and the number of non-zero parameters (#prms) of the trained networks.

Second, we compute an approximate number of adversarial examples for a given image. We used 4 hidden layers and one output layer. The input of the network is an image of size 28×28 . The network has the following dimensions for all layers: [784, 500, 300, 200, 100, 10]. This gives 623K parameters, which is 3 to 10 times bigger than the networks in (Narodytska et al., 2018; Baluta et al., 2019). We used a full-precision trained network to seed weights before binarized training (Alizadeh et al., 2019). As the first layer inputs are reals, we used an additional BN + sign layer after the input layer to binarize inputs (see Appendix D.1). We used the PySAT tool (Ignatiev et al., 2018) to encode logical constraints to SAT and Glucose as a SAT solver (Audemard & Simon, 2018).

Untargeted adversarial attacks. In this task, we look for a perturbation x' of the given input x where $|x - x'| \leq \epsilon$. We used five values of epsilon, $\epsilon \in \{1, 3, 5, 10, 15, 20\}^4$. We train three groups of networks. First, we trained vanilla BNNs. Then we trained two types of BNNs using our ideas from the neuron level. We trained BNNs with the ternary quantization method ('Sparse'). We used the value of $T = 0.03$ for MNISTBG and FASHION and $T = 0.04$ for MNIST using 60%-80% quantile depending on the dataset and the accuracy of the resulting network. Finally, we trained BNNs with stabilization of neurons ('Sparse+Stable'). We seeded initial weights of 'Sparse+Stable' network with weights of the trained 'Sparse' network as such a setup up gave better accuracy. In addition, we investigate the effect of a popular L1 regularizer on ternary quantization during the training ('Sparse+L1') and its stabilization version ('Sparse+L1+Stable').

Table 2 summarizes test accuracy results and the number of non-zero parameters per network for all trained networks and datasets. From Table 2, we can see that we can significantly reduce the number of parameters using ternary quantization during the training ('Sparse'). Interestingly, we do not lose test accuracy compared to the vanilla BNNs in all cases. If we consider the effect of L1 regularization then we see that the number of parameters reduces even further but the accuracy drops a bit as well: the more we reduce the number of non-zero parameters the more we lose in terms of the accuracy. Using additional stabilization can also hurt the accuracy a bit for both 'Sparse' and 'Sparse+L1' networks. However, on average, we get about 40% of signs stabilized.

Figure 1 shows the performance of a SAT solver on three datasets. Results are averaged over 100 benchmarks. The average size of the encoding for all datasets and $\epsilon = 5$ are shown in Table 3. Note that the size of the encoding is 50x smaller compared to millions of variables and classes reported in Narodytska et al. (2018) for MNIST and MNISTBG for a much smaller network and the same ϵ . Another interesting observation is that stabilization helps a lot to reduce the size of the encoding. If the PySAT tool takes more than 10G of memory to generate a SAT encoding then we terminate the generation process. If a solver time/memory outs on more than 70% of benchmarks we do not plot these results. Therefore, we do not have a plot for vanilla BNNs in these datasets as we either had a timeout or (mostly) memory out exceptions. Each plot shows the average time to solve the untargeted adversarial attack problem for each value of ϵ . In all except one case, at least 95% of benchmarks were solved within the 100 sec timeout (See Appendix D.2, Figure 3 for details on the number of solved instances.). The plots show that ternary quantization greatly improves performance on three datasets as we were not even able to solve any benchmarks for the vanilla case. Using the 'L1' regularizer slightly improves performance in two datasets and helps a lot on MNIST. Finally, the stabilization of signs method consistently improves performance of a SAT solver across datasets for both 'Sparse' and 'Sparse+L1' networks, e.g. we get from 3x to 6x speedup due to stabilization.

Figure 2 shows the number of successful attacks as it is an interesting measure to understand properties of a network. Each plot shows the ratio of successful adversarial attacks for each value of ϵ . Naturally, this ratio plateaus at 1 as the value of perturbation ϵ grows. The results are mixed here. In some cases, using 'L1' does not significantly change the vulnerability of the network compared to 'Sparse' network, e.g. FASHION and MNISTBG, while it does help for MNIST. Interestingly,

⁴We are able to use large values of ϵ compared to Narodytska et al. (2018), where $\epsilon \leq 5$.

BNNs	MNIST			FASHION			MNISTBG		
	#vars/#cls	P(adv)	#solved	#vars/#cls	P(adv)	#solved	#vars/#cls	P(adv)	#solved
Sparse	63K/224K	0.04	71%	34K/116K	0.04	87%	24K/80K	0.17	95%
Sparse+Stable	42K/146K	0.05	70%	19K/58K	0.06	89%	12K/36K	0.16	93%
Sparse+L1	8K/20K	0.07	100%	34K/115K	0.07	87%	17K/53K	0.17	98%
Sparse+Stable+L1	11K/33K	0.05	95%	12K/33K	0.06	98%	10K/28K	0.16	94%

Table 3: The average size of the SAT encoding in terms of the number of variables (#vars) and clauses (#cls), the probability of perturbation to be an adversarial attack(P(adv)) and the number of solved benchmarks out all of benchmarks that can be attacked for $\epsilon = 5$.

stabilization of signs can lead to increase in vulnerabilities if we compare a network with and without stabilization. Consider for example, MNIST with $\epsilon = 5$. Only 13 out of 100 benchmarks were successfully attacked for ‘Sparse+L1’ while 43 were attacked for ‘Sparse+L1+Stable’.

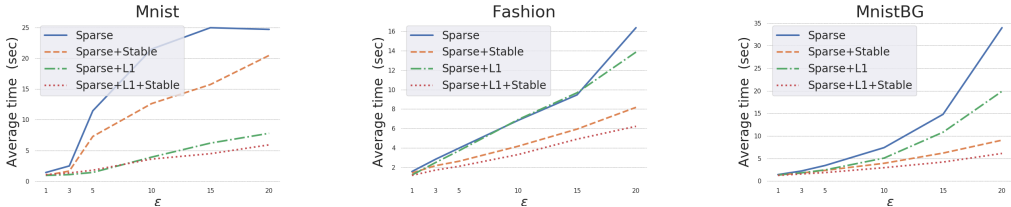


Figure 1: Performance of a SAT solver on the untargeted adversarial attack task.

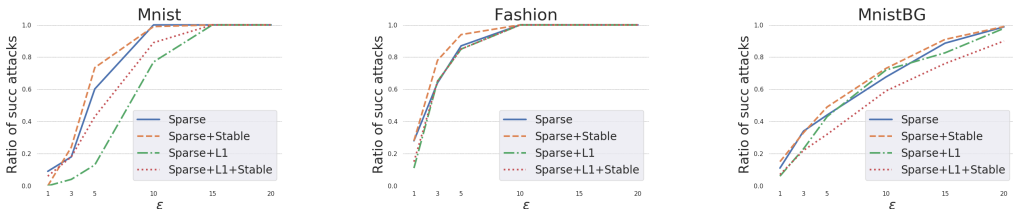


Figure 2: The percentage of successful adversarial attacks.

Likelihood of adversarial examples. Next we estimate the probability of a perturbation to be an adversarial example. We reproduce a setup from (Baluta et al., 2019) where an approximate model counting, ApproxMC3, was used to perform such estimate. The main goal of this experiment is to demonstrate that our approach allows approximate model counting techniques to scale to larger networks. We focus on robustness as above, so SAT formulas check for existence of untargeted adversarial attacks. Hence, each solution corresponds to an adversarial attack. We perform model counting on binarized inputs (see Appendix D.1) with a timeout of 600 sec. We use default parameters of ApproxMC3. Table 3 summarizes results. We report the mean value of the solution count estimate divided by the total number of solutions (P(adv)) and the percentage of benchmarks solved by ApproxMC3 out of all benchmarks that we know are susceptible to adversarial perturbation (#solved). On average, we can solve 80% of benchmarks within the timeout. This contrasts with results reported in (Baluta et al., 2019), where it took 24 hours to perform approximate model counting for a BNN with about 50K parameters and a large fraction of benchmarks were not solved. Table 3 shows that the probability of adversarial attack is small for two out of three datasets.

In summary, our results show that a significant speed up can be obtained if we design an architecture of BNNs and its training procedure taking into account potential bottlenecks of SAT solvers. For completeness of the evaluation, we report results of an ILP solver on the same benchmarks for the untargeted adversarial attacks (Appendix D.3). The second experiment is not currently possible for ILP formulations as we are not aware of an efficient approximate model counting solver for ILPs.

7 CONCLUSIONS

In this work, we analyze architectural design choices of BNNs and discuss how they affect the performance of logic-based reasoners, focusing on the individual neuron and block levels. We demonstrated how to train BNNs so that the resulting network is easier to verify for logic-based engines, like SAT solver or approximate model counting solvers.

REFERENCES

- Milad Alizadeh, Javier Fernández-Marqués, Nicholas D. Lane, and Yarin Gal. An empirical study of binary neural networks’ optimisation. In *7th International Conference on Learning Representations, ICLR 2019, New Orleans, LA, USA, May 6-9, 2019*. OpenReview.net, 2019. URL <https://openreview.net/forum?id=rJfUCoR5KX>.
- Gilles Audemard and Laurent Simon. On the glucose SAT solver. *International Journal on Artificial Intelligence Tools*, 27(1):1–25, 2018. doi: 10.1142/S0218213018400018. URL <https://doi.org/10.1142/S0218213018400018>.
- Teodora Baluta, Shiqi Shen, Shweta Shinde, Kuldeep S. Meel, and Prateek Saxena. Quantitative verification of neural networks and its security applications. *ACM Conference on Computer and Communications Security (CCS 2019)*, abs/1906.10395, 2019. URL <http://arxiv.org/abs/1906.10395>.
- Armin Biere, Marijn Heule, Hans van Maaren, and Toby Walsh (eds.). *Handbook of Satisfiability*, volume 185 of *Frontiers in Artificial Intelligence and Applications*. IOS Press, 2009. ISBN 978-1-58603-929-5.
- Aaron R. Bradley. Sat-based model checking without unrolling. In Ranjit Jhala and David A. Schmidt (eds.), *Verification, Model Checking, and Abstract Interpretation - 12th International Conference, VMCAI 2011, Austin, TX, USA, January 23-25, 2011. Proceedings*, volume 6538 of *Lecture Notes in Computer Science*, pp. 70–87. Springer, 2011. doi: 10.1007/978-3-642-18275-4_7. URL https://doi.org/10.1007/978-3-642-18275-4_7.
- Supratik Chakraborty, Kuldeep S. Meel, and Moshe Y. Vardi. A scalable approximate model counter. In Christian Schulte (ed.), *Principles and Practice of Constraint Programming - 19th International Conference, CP 2013, Uppsala, Sweden, September 16-20, 2013. Proceedings*, volume 8124 of *Lecture Notes in Computer Science*, pp. 200–216. Springer, 2013.
- Chih-Hong Cheng, Georg Nührenberg, Chung-Hao Huang, and Harald Ruess. Verification of binarized neural networks via inter-neuron factoring - (short paper). In Ruzica Piskac and Philipp Rümmer (eds.), *Verified Software. Theories, Tools, and Experiments - 10th International Conference, VSTTE 2018, Oxford, UK, July 18-19, 2018, Revised Selected Papers*, volume 11294 of *Lecture Notes in Computer Science*, pp. 279–290. Springer, 2018. doi: 10.1007/978-3-030-03592-1_16. URL https://doi.org/10.1007/978-3-030-03592-1_16.
- Arthur Choi, Weijia Shi, Andy Shih, and Adnan Darwiche. Compiling neural networks into tractable boolean circuits. 2019.
- Tri Dao, Albert Gu, Matthew Eichhorn, Megan Leszczynski, Nimit Sohoni, Amit Blonder, Atri Rudra, and Chris Ré. Butterflies are all you need: A universal building block for structured linear maps. 2019a. URL <https://dawn.cs.stanford.edu/2019/06/13/butterfly/>.
- Tri Dao, Albert Gu, Matthew Eichhorn, Atri Rudra, and Christopher Ré. Learning fast algorithms for linear transforms using butterfly factorizations. In Kamalika Chaudhuri and Ruslan Salakhutdinov (eds.), *Proceedings of the 36th International Conference on Machine Learning, ICML 2019, 9-15 June 2019, Long Beach, California, USA*, volume 97, pp. 1517–1527, 2019b.
- Sajad Darabi, Mouloud Belbahri, Matthieu Courbariaux, and Vahid Partovi Nia. BNN+: improved binary network training. *CoRR*, abs/1812.11800, 2018. URL <http://arxiv.org/abs/1812.11800>.
- Krishnamurthy Dvijotham, Sven Gowal, Robert Stanforth, Relja Arandjelovic, Brendan O’Donoghue, Jonathan Uesato, and Pushmeet Kohli. Training verified learners with learned verifiers. *CoRR*, abs/1805.10265, 2018. URL <http://arxiv.org/abs/1805.10265>.
- Stefano Ermon, Carla P. Gomes, Ashish Sabharwal, and Bart Selman. Taming the curse of dimensionality: Discrete integration by hashing and optimization. In *Proceedings of the 30th International Conference on Machine Learning, ICML 2013, Atlanta, GA, USA, 16-21 June 2013*, volume 28, pp. 334–342. JMLR.org, 2013.
- EU Data Protection Regulation. Regulation (EU) 2016/679 of the European Parliament and of the Council, 2016.

- Ian Goodfellow, Yoshua Bengio, and Aaron Courville. *Deep Learning*. The MIT Press, 2016. ISBN 0262035618, 9780262035613.
- Ian J Goodfellow, Jonathon Shlens, and Christian Szegedy. Explaining and harnessing adversarial examples. In *ICLR’15*, 2015.
- Bryce Goodman and Seth R. Flaxman. European Union regulations on algorithmic decision-making and a ”right to explanation”. *AI Magazine*, 38(3):50–57, 2017.
- Arie Gurfinkel, Temesghen Kahsai, Anvesh Komuravelli, and Jorge A. Navas. The seahorn verification framework. In Daniel Kroening and Corina S. Pasareanu (eds.), *Computer Aided Verification - 27th International Conference, CAV 2015, San Francisco, CA, USA, July 18-24, 2015, Proceedings, Part I*, volume 9206 of *Lecture Notes in Computer Science*, pp. 343–361. Springer, 2015. doi: 10.1007/978-3-319-21690-4_20. URL https://doi.org/10.1007/978-3-319-21690-4_20.
- Itay Hubara, Matthieu Courbariaux, Daniel Soudry, Ran El-Yaniv, and Yoshua Bengio. Binarized Neural Networks. In *Advances in Neural Information Processing Systems 29*, pp. 4107–4115. Curran Associates, Inc., 2016. URL <http://papers.nips.cc/paper/6573-binarized-neural-networks.pdf>.
- Alexey Ignatiev, Antonio Morgado, and Joao Marques-Silva. PySAT: A Python toolkit for prototyping with SAT oracles. In *SAT*, pp. 428–437, 2018. doi: 10.1007/978-3-319-94144-8_26. URL https://doi.org/10.1007/978-3-319-94144-8_26.
- Sergey Ioffe and Christian Szegedy. Batch Normalization: Accelerating Deep Network Training by Reducing Internal Covariate Shift. *Arxiv*, 2015. ISSN 0717-6163. doi: 10.1007/s13398-014-0173-7.2.
- Guy Katz, Clark W. Barrett, David L. Dill, Kyle Julian, and Mykel J. Kochenderfer. Reluplex: An efficient SMT solver for verifying deep neural networks. In *CAV*, pp. 97–117, 2017.
- Guy Katz, Derek A. Huang, Duligur Ibeling, Kyle Julian, Christopher Lazarus, Rachel Lim, Parth Shah, Shantanu Thakoor, Haoze Wu, Aleksandar Zeljic, David L. Dill, Mykel J. Kochenderfer, and Clark W. Barrett. The Marabou framework for verification and analysis of deep neural networks. In *CAV*, pp. 443–452, 2019.
- Elias B. Khalil, Amrita Gupta, and Bistra Dilkina. Combinatorial attacks on binarized neural networks. In *7th International Conference on Learning Representations, ICLR 2019, New Orleans, LA, USA, May 6-9, 2019*. OpenReview.net, 2019. URL <https://openreview.net/forum?id=S1lTEh09FQ>.
- Jaeha Kung, David Zhang, Gooitzen Van der Wal, Sek Chai, and Saibal Mukhopadhyay. Efficient Object Detection Using Embedded Binarized Neural Networks. *Journal of Signal Processing Systems*, pp. 1–14, 2017.
- Jean-Marie Lagniez and Pierre Marquis. An improved decision-dnnf compiler. In *IJCAI*, pp. 667–673, 2017.
- Bradley McDanel, Surat Teerapittayanon, and H. T. Kung. Embedded binarized neural networks. In *EWSN*, pp. 168–173. Junction Publishing, Canada / ACM, 2017.
- Matthew Mirman, Timon Gehr, and Martin T. Vechev. Differentiable abstract interpretation for provably robust neural networks. In Jennifer G. Dy and Andreas Krause (eds.), *Proceedings of the 35th International Conference on Machine Learning, ICML 2018, Stockholm, Sweden, July 10-15, 2018*, volume 80 of *Proceedings of Machine Learning Research*, pp. 3575–3583. PMLR, 2018. URL <http://proceedings.mlr.press/v80/mirman18b.html>.
- Christian Muise, Sheila A. McIlraith, J. Christopher Beck, and Eric Hsu. DSHARP: Fast d-DNNF Compilation with sharpSAT. In *Canadian Conference on Artificial Intelligence*, 2012.
- Nina Narodytska, Shiva Prasad Kasiviswanathan, Leonid Ryzhyk, Mooly Sagiv, and Toby Walsh. Verifying properties of binarized deep neural networks. In Sheila A. McIlraith and Kilian Q. Weinberger (eds.), *Proceedings of the Thirty-Second AAAI Conference on Artificial Intelligence, (AAAI-18), 2-7, 2018*, pp. 6615–6624. AAAI Press, 2018. URL <https://www.aaai.org/ocs/index.php/AAAI/AAAI18/paper/view/16898>.

- Nina Narodytska, Aditya A. Shrotri, Kuldeep S. Meel, Alexey Ignatiev, and João Marques-Silva. Assessing heuristic machine learning explanations with model counting. In Mikolás Janota and Inês Lynce (eds.), *Theory and Applications of Satisfiability Testing - SAT 2019 - 22nd International Conference, SAT 2019*, volume 11628 of *Lecture Notes in Computer Science*, pp. 267–278. Springer, 2019.
- NIPS IML Symposium. NIPS interpretable ML symposium, December 2017.
- Aditi Raghunathan, Jacob Steinhardt, and Percy Liang. Semidefinite relaxations for certifying robustness to adversarial examples. In *Advances in Neural Information Processing Systems 31: Annual Conference on Neural Information Processing Systems 2018, NeurIPS 2018, 3-8 December 2018, Montréal, Canada.*, pp. 10900–10910, 2018.
- T. Sang, P. Beame, and H. Kautz. Performing bayesian inference by weighted model counting. In *Prof. of AAAI*, pp. 475–481, 2005.
- Andy Shih, Adnan Darwiche, and Arthur Choi. Verifying binarized neural networks by anguin-style learning. In Mikolás Janota and Inês Lynce (eds.), *Theory and Applications of Satisfiability Testing - SAT 2019 - 22nd International Conference, SAT 2019*, volume 11628 of *Lecture Notes in Computer Science*, pp. 354–370. Springer, 2019.
- Gagandeep Singh, Timon Gehr, Matthew Mirman, Markus Püschel, and Martin T. Vechev. Fast and effective robustness certification. In *NeurIPS*, pp. 10825–10836, 2018. URL <http://papers.nips.cc/paper/8278-fast-and-effective-robustness-certification>.
- Gagandeep Singh, Timon Gehr, Markus Püschel, and Martin T. Vechev. Boosting robustness certification of neural networks. In *7th International Conference on Learning Representations, ICLR 2019, New Orleans, LA, USA, May 6-9, 2019*. OpenReview.net, 2019. URL <https://openreview.net/forum?id=HJgeEh09KQ>.
- Carsten Sinz. Towards an optimal CNF encoding of boolean cardinality constraints. In *CP*, volume 3709 of *Lecture Notes in Computer Science*, pp. 827–831. Springer, 2005a.
- Carsten Sinz. Towards an optimal CNF encoding of boolean cardinality constraints. Technical report, University of Tübingen, 2005b.
- Mate Soos and Kuldeep S. Meel. Bird: Engineering an efficient cnf-xor sat solver and its applications to approximate model counting. In *Proceedings of AAAI Conference on Artificial Intelligence (AAAI)*, 1 2019.
- Mate Soos, Karsten Nohl, and Claude Castelluccia. Extending SAT solvers to cryptographic problems. In *Theory and Applications of Satisfiability Testing - SAT 2009, 12th International Conference, SAT 2009, Swansea, UK, June 30 - July 3, 2009. Proceedings*, pp. 244–257, 2009.
- Marc Thurley. sharpsat - counting models with advanced component caching and implicit BCP. In Armin Biere and Carla P. Gomes (eds.), *Theory and Applications of Satisfiability Testing - SAT 2006, 9th International Conference, Seattle, WA, USA, August 12-15, 2006, Proceedings*, volume 4121 of *Lecture Notes in Computer Science*, pp. 424–429. Springer, 2006. doi: 10.1007/11814948_38. URL https://doi.org/10.1007/11814948_38.
- Vincent Tjeng, Kai Y. Xiao, and Russ Tedrake. Evaluating robustness of neural networks with mixed integer programming. In *ICLR*, 2019.
- Leslie G. Valiant. The complexity of enumeration and reliability problems. *SIAM J. Comput.*, 8(3): 410–421, 1979. doi: 10.1137/0208032. URL <https://doi.org/10.1137/0208032>.
- Leslie G Valiant. A theory of the learnable. In *Proceedings of the sixteenth annual ACM symposium on Theory of computing*, pp. 436–445. ACM, 1984.
- Tsui-Wei Weng, Huan Zhang, Hongge Chen, Zhao Song, Cho-Jui Hsieh, Luca Daniel, Duane S. Boning, and Inderjit S. Dhillon. Towards fast computation of certified robustness for relu networks. In *ICML*, pp. 5273–5282, 2018.

Eric Wong and J. Zico Kolter. Provable defenses against adversarial examples via the convex outer adversarial polytope. In Jennifer G. Dy and Andreas Krause (eds.), *Proceedings of the 35th International Conference on Machine Learning, ICML 2018, Stockholmsmässan, Stockholm, Sweden, July 10-15, 2018*, volume 80 of *Proceedings of Machine Learning Research*, pp. 5283–5292. PMLR, 2018. URL <http://proceedings.mlr.press/v80/wong18a.html>.

Kai Y. Xiao, Vincent Tjeng, Nur Muhammad (Mahi) Shafiullah, and Aleksander Madry. Training for faster adversarial robustness verification via inducing relu stability. In *7th International Conference on Learning Representations, ICLR 2019, New Orleans, LA, USA, May 6-9, 2019*. OpenReview.net, 2019. URL <https://openreview.net/forum?id=BJfIVjAcKm>.

Huan Zhang, Tsui-Wei Weng, Pin-Yu Chen, Cho-Jui Hsieh, and Luca Daniel. Efficient neural network robustness certification with general activation functions. In *NeurIPS*, pp. 4944–4953, 2018.

Chenzhuo Zhu, Song Han, Huizi Mao, and William J. Dally. Trained ternary quantization. In *5th International Conference on Learning Representations, ICLR 2017, Toulon, France, April 24-26, 2017, Conference Track Proceedings*. OpenReview.net, 2017. URL https://openreview.net/forum?id=S1_pAu9xl.

A BACKGROUND. ADDITIONAL DETAILS.

Model counting. The problem of model counting is to calculate the number satisfying assignments or models of a given SAT formula. This problem is complete for the complexity class $\#\mathcal{P}$ (Valiant, 1979), which contains the entire polynomial hierarchy. Despite the high complexity, a number of tools for model counting have been developed (Sang et al., 2005; Thurley, 2006; Muise et al., 2012; Lagniez & Marquis, 2017), which were shown to work well on certain benchmarks arising in practice. However, for many applications, obtaining exact counts is not necessary and a good approximation often suffices, especially when it leads to better scalability. These requirements have led to the emergence of *approximate* counting approaches (Ermon et al., 2013; Chakraborty et al., 2013; Soos & Meel, 2019) which employ universal hash functions along with specialized SAT solvers (Soos et al., 2009) for balancing accuracy and scalability. The most successful approximate counters provide Probabilistically Approximately Correct (PAC)-style guarantees (Valiant, 1984) on accuracy, while scaling to formulas with thousands of variables in practice. In our experiments, we use a state-of-the-art tool called ApproxMC3 (Soos & Meel, 2019) which has been shown to scale much better than other exact and approximate counters. A key advantage of ApproxMC3 is that it supports *projected* model counting, i.e. counting over a subset of the variables in the given formula, which is essential for our purposes as we count over variables that represent inputs of the network.

Sequential counters encoding. We recall the definition of *sequential counters* encoding from (Sinz, 2005a;b) that are used to encode cardinality constraints. Consider a cardinality constraint: $\sum_{i=1}^m l_i \geq k$, where $l_i \in \{0, 1\}$ is a Boolean variable, \mathbf{x}_i , or its negation, $\bar{\mathbf{x}}_i$, and k is a constant. Then the sequential counter encoding, can be written as the following Boolean formula using auxiliary Boolean variables $r_{(j,k)}$:

$$\begin{aligned} & (l_1 \Leftrightarrow r_{(1,1)}) \wedge (\bar{r}_{(1,j)}, j \in \{2, \dots, k\}) \wedge \\ & \quad r_{(i,1)} \Leftrightarrow l_i \vee r_{(i-1,1)} \wedge \\ & r_{(i,j)} \Leftrightarrow l_i \wedge r_{(i-1,j-1)} \vee r_{(i-1,j)}, j \in \{2, \dots, k\}, \end{aligned} \tag{5}$$

where $i \in \{2, \dots, m\}$. Essentially, this encoding computes the cumulative sums $\sum_{i=1}^k l_i$ and the computation is performed in unary, i.e., the Boolean variable $r_{(j,k)}$ is true iff $\sum_{i=1}^j l_i \geq k$. In particular, $r_{(m,k)}$ encodes whether $\sum_{i=1}^m l_i$ is greater than or equal to k .

B ENCODING OF THE OUTPUT LAYER AND ITS ADJUSTMENT FOR TERNARY QUANTIZATION

We recall that the OUTPUT block is just a linear transformation: $o = Cx^{d-1} + q$.

Example B.1. We continue Example 3.1. Suppose our single block is followed by an output block with two inputs and two outputs. We define transformation parameters as follows.

$$\text{LIN} : C = [1, -1; -1, -1], q = [0.5, -0.1] \quad (6)$$

Hence, we can write the following system of linear constraints over $\{-1, 1\}$ variables.

$$\begin{aligned} o_0 &= x_0^1 - x_1^1 + 0.5, \\ o_1 &= -x_0^1 - x_1^1 - 0.1. \end{aligned}$$

As before, we perform variable replacement to obtain constraints over Boolean variables only.

$$\begin{aligned} o_0 &= 2\mathbf{x}_0^1 - 1 - (2\mathbf{x}_1^1 - 1) + 0.5, \\ o_1 &= -(2\mathbf{x}_0^1 - 1) - (2\mathbf{x}_1^1 - 1) - 0.1. \end{aligned}$$

After rearrangements, we get

$$\begin{aligned} o_0 &= 2\mathbf{x}_0^1 - 2\mathbf{x}_1^1 + 0.5, \\ o_1 &= -2\mathbf{x}_0^1 - 2\mathbf{x}_1^1 + 1.9. \quad \square \end{aligned}$$

Usually, we are not interested in absolute values of o . Rather, we need to know the index of the maximum element of o , which corresponds to the top prediction in the classification task. Hence, we need to encode the ordering relation over variables o . To do so, we use an additional set of Boolean variables $d_{ij}, i = 1, \dots, p, j = i + 1, \dots, p$. Applying variable replacements and rearranging terms, we get:

$$d_{ij} \Leftrightarrow \left(\sum_{t=1}^p c_{it} 2\mathbf{x}_t^d - \sum_{t=1}^p c_{it} + q_i \geq \sum_{t=1}^p c_{jt} 2\mathbf{x}_t^d - \sum_{t=1}^p c_{jt} + q_j \right) \quad (7)$$

$$\text{we denote } R_{ij} = \left(\sum_{t=1}^p c_{it} - q_i - \sum_{t=1}^p c_{jt} + q_j \right), \text{ so we get} \quad (8)$$

$$\Leftrightarrow \left(\sum_{t=1}^p c_{it} \mathbf{x}_t^d - \sum_{t=1}^p c_{jt} \mathbf{x}_t^d \geq \frac{R_{ij}}{2} \right) \quad (9)$$

$$\Leftrightarrow \left(\sum_{t=1}^p (c_{it} - c_{jt}) \mathbf{x}_t^d \geq \frac{R_{ij}}{2} \right) \quad (10)$$

Finally, we note that $c_{it}, c_{jt} \in \{-1, 1\}$ are applied to the same variable x_t^d . Hence, depending on the sign of these coefficients, the difference $|c_{it} - c_{jt}|$ is either 0 or 2. So we can rewrite:

$$d_{ij} \Leftrightarrow \left(2 \times \sum_{t=1, c_{it}-c_{jt}=2}^p \mathbf{x}_t^d - 2 \times \sum_{t=1, c_{it}-c_{jt}=-2}^p \mathbf{x}_t^d \geq \frac{R_{ij}}{2} \right) \quad (11)$$

$$\Leftrightarrow \left(\sum_{t=1, c_{it}-c_{jt}=2}^p \mathbf{x}_t^d - \sum_{t=1, c_{it}-c_{jt}=-2}^p \mathbf{x}_t^d \geq \left\lceil \frac{R_{ij}}{4} \right\rceil \right) \quad (12)$$

Example B.2. Coming back to our Example B.1, as we have two variables, we introduce one Boolean variable d_{01} to signal the top prediction:

$$\begin{aligned} d_{0,1} &\Leftrightarrow o_0 \geq o_1 \\ &\Leftrightarrow (2\mathbf{x}_0^1 - 2\mathbf{x}_1^1 + 2\mathbf{x}_0^1 + 2\mathbf{x}_1^1 \geq 1.9 - 0.5) \\ &\Leftrightarrow (\mathbf{x}_0^1 - \mathbf{x}_1^1 + \mathbf{x}_0^1 + \mathbf{x}_1^1 \geq 1.4/2) \\ &\Leftrightarrow \mathbf{x}_0^1 \geq \lceil 1.4/4 \rceil \quad \square \end{aligned}$$

The final observation is that if C is a sparse matrix then we lose the property that the difference $c_{it} - c_{jt}$ is either 0 or 2 as $c_{it}, c_{jt} \in \{-1, 0, 1\}$. Hence, the last division by two (Equation 12) is not possible. However, we take advantage of the fact that coefficients are small, $|c_{it} - c_{jt}| \leq 2$. So, we can duplicate variables to model non-unary coefficients, for example.

Example B.3. Suppose, we get the following matrix C due to ternary quantization:

$$\text{LIN} : C = [1, 0; -1, -1], q = [0.5, -0.1] \quad (13)$$

Then we have the following ordering constraint:

$$\begin{aligned} d_{0,1} &\Leftrightarrow o_0 \geq o_1 \\ &\Leftrightarrow (2\mathbf{x}_0^1 - 1 + 0.5 \geq -2\mathbf{x}_0^1 + 1 - 2\mathbf{x}_1^1 + 1 - 0.1) \\ &\Leftrightarrow (\mathbf{x}_0^1 + \mathbf{x}_0^1 + \mathbf{x}_1^1 \geq 2.4/2) \\ &\Leftrightarrow 2\mathbf{x}_0^1 + \mathbf{x}_1^1 \geq \lceil 2.4/2 \rceil \end{aligned}$$

We can introduce an extra variable $\mathbf{x}_0^{1'}$ and replace $2\mathbf{x}_0^1 + \mathbf{x}_1^1$ with $\mathbf{x}_0^1 + \mathbf{x}_0^{1'} + \mathbf{x}_1^1$ and an equality constraint $\mathbf{x}_0^1 = \mathbf{x}_0^{1'}$. \square

C BOUNDS PROPAGATION

Let us split BLOCK computation into two parts that correspond to LIN and BN layers: $y_j^i = \sum_{t=1}^{n_i} a_{j,t}^i x_t^i + b_j^i$ and $z_j^i = \frac{\alpha_j^i}{\sigma_j^i} (y_j^i - \mu_j^i) + \gamma_j^i$ to demonstrate computations of lower and upper bounds on y_j^i (z_j^i are computed similarly). We get that

$$lb(y_j^i) = \sum_{t=1, a_{j,t}^i > 0}^{n_i} a_{j,t}^i lb(x_t^i) + \sum_{t=1, a_{j,t}^i < 0}^{n_i} a_{j,t}^i ub(x_t^i) + b_j^i \quad (14)$$

$$ub(y_j^i) = \sum_{t=1, a_{j,t}^i > 0}^{n_i} a_{j,t}^i ub(x_t^i) + \sum_{t=1, a_{j,t}^i < 0}^{n_i} a_{j,t}^i lb(x_t^i) + b_j^i \quad (15)$$

Example C.1. Consider our example for BLOCK and the second neuron computation:

$$x_1^1 = \text{sign}(0.1(-x_0^0 - x_1^0 + x_2^0 + 1) + 0.2 \geq 0).$$

Suppose we derive that for all possible samples, $ub(x_0^0) = ub(x_1^0) = -1$. In this case, we have $lb(x_0^0) = lb(x_1^0) = -1$ as all activations are in $\{-1, 1\}$. We can compute bounds on the all variables y and z .

$$\begin{aligned} lb(y_1^1) &= lb(-x_0^0 - x_1^0 + x_2^0) = 1 + 1 - 1 = 1, \\ ub(y_1^1) &= ub(-x_0^0 - x_1^0 + x_2^0) = 1 + 1 + 1 = 3, \\ lb(z_1^1) &= 0.1 \times lb(y_1^1 + 1) + 0.2 = 0.4, \\ ub(z_1^1) &= 0.1 \times ub(y_1^1 + 1) + 0.2 = 0.6. \end{aligned}$$

So, we get that $\text{sign}(lb(z_1^1)) = \text{sign}(ub(z_1^1))$, so we know that $x_1^1 = 1$ and we can use this information to reduce the encodings. \square

D EXPERIMENTAL EVALUATION.

D.1 BINARIZATION OF INPUTS.

As we discussed in Section 6, we introduce an additional block before the first internal layer that mimics binarization of inputs. This layer constraints BN and sign operators only (hard tanh is used during the training). Consider how this layer works.

$$\mathbf{x}_t^0 \Leftrightarrow \text{sign} \left(\frac{\alpha_t}{\sigma_t} (x'_t + b_t - \mu_t) + \gamma_t \right),$$

$$x'_t \in [x_t - \epsilon, x_t + \epsilon].$$

First, we consider two extreme values of the expression that is an input of sign w.r.t. ϵ . Suppose $\alpha_t \geq 0$ ($\alpha_t < 0$ is analogous).

$$\max_t = \frac{\alpha_t}{\sigma_t} (x_t + \epsilon + b_t - \mu_t) + \gamma_t, \quad (16)$$

$$\min_t = \frac{\alpha_t}{\sigma_t} (x_t - \epsilon + b_t - \mu_t) + \gamma_t \quad (17)$$

If $\min_t \geq 0$ then we know that $\mathbf{x}_t^0 = 1$. If $\max_j < 0$ then we know that $\mathbf{x}_t^0 = 0$. In other cases, $\mathbf{x}_t^0 \in \{0, 1\}$. Consider the reverse transformation. If $\mathbf{x}_j^0 = 0$ is a solution of a problem produced by the SAT solver then we can map back to $x_t = \min_t$. Similarly, if $\mathbf{x}_t^0 = 1$ then $x_t = \max_t$. As each transformation in Equation 16–Equation 17 is performed on a single input, we can build a valid input from a solution over Boolean variables.

D.2 EXPERIMENTAL EVALUATION USING SAT SOLVERS.

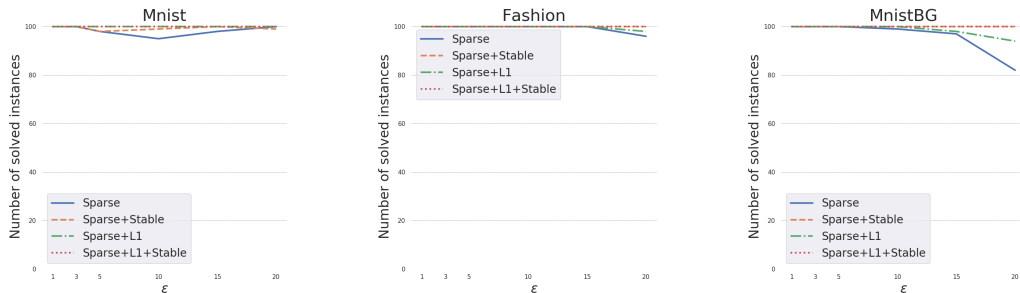


Figure 3: The number of solved benchmarks.

Number of solved benchmarks. Figure 3 shows the number of solved problems for each ϵ value within the timeout by the SAT solver. As can be seen from these plots, in all except one case, at least 95% of benchmarks were solved with the 100 sec timeout.

Examples of perturbed images. Table 4 shows original (the top row) and perturbed (the bottom row) samples of images for $\epsilon = 3, 5, 15, 20$ (from left to right). As can be seen from these sample, if $\epsilon = 3$ then original and perturbed images are identical. For $\epsilon = 20$ (last column), perturbations are visible.



Table 4: The original (the top row) and successfully perturbed (the bottom row) images for MNISTBG for $\epsilon = 3, 5, 15, 20$.

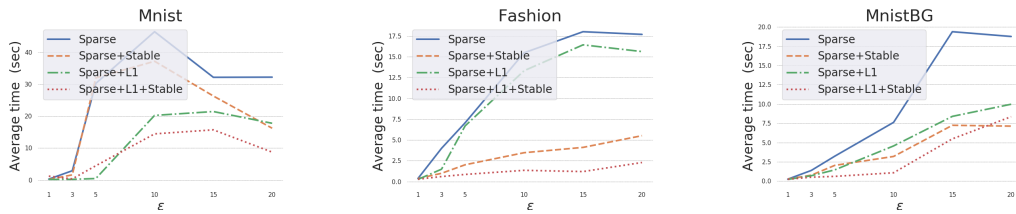


Figure 4: Performance of an ILP solver on the untargeted adversarial attack task.

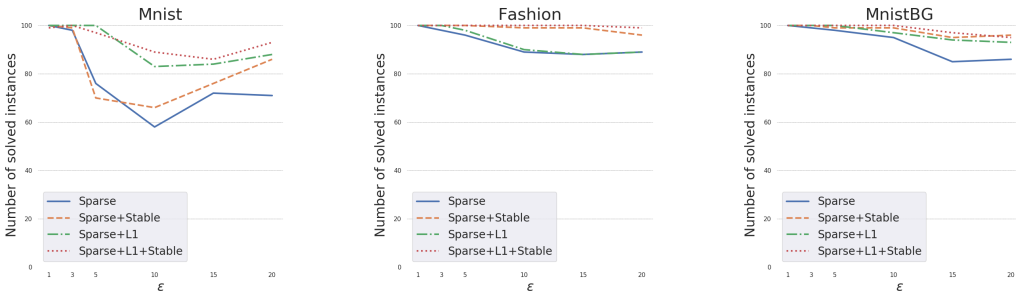


Figure 5: The number of solved benchmarks.

D.3 EXPERIMENTAL EVALUATION USING ILP SOLVERS.

We present results solving the benchmarks from Section 6 using an ILP solver. We used the CPLEX solver with default configuration. Figure 4–Figure 5 shows our results. As in Section 6, Figure 4 shows the performance of a SAT solver on the untargeted adversarial example task for each value of ϵ . Results are averaged over 100 benchmarks. We observe similar patterns as in Section 6: sparsification and stabilization are mostly helpful for all datasets as we cannot solve most of the benchmarks if we do not apply these techniques. Also, Figure 5 shows the number of solved problems for each ϵ value within the timeout. As can be seen from the graph, the ILP solver exhibits a bell shape in two datasets, MNIST and FASHION: if ϵ is small or large then the instance is easier to solve. ϵ values in the middle are the hardest to solve for an ILP solver. We have not observed this bell shape for SAT solvers. Overall, if we compare performance of SAT and ILP solvers, the SAT solver is more efficient and solves more benchmarks.